J. Membrane Biol. 189, 67–81 (2002)
DOI: 10.1007/s00232-001-0190-2

The Journal of
Membrane
Biology

Mechanisms of Activation of NHE by Cell Shrinkage and by Calyculin A in Ehrlich Ascites Tumor Cells

S.F. Pedersen*, C. Varming*, S.T. Christensen, E.K. Hoffmann
Department of Biochemistry, August Krogh Institute, University of Copenhagen, 13, Universitetsparken, DK-2100 Copenhagen, Denmark

Received: 5 December 2001/Revised: 2 May 2002

Abstract. The Na^+/H^+ exchanger isoforms NHE1, NHE2, and NHE3 were all found to be expressed in Ehrlich ascites tumor cells, as evaluated by Western blotting and confocal microscopy. Under unstimulated conditions, NHE1 was found predominantly in the plasma membrane, NHE3 intracellularly, and NHE2 in both compartments. Osmotic cell shrinkage elicited a rapid intracellular alkalinization, the sensitivity of which to EIPA (IC_{50} 0.19 μM) and HOE 642 (IC_{50} 0.85 μM) indicated that it predominantly reflected activation of NHE1. NHE activation by osmotic shrinkage was inhibited by the protein kinase C inhibitors chelerythrine (IC_{50} 12.5 μM), Gö 6850 (5 μM), and Gö 6976 (1 μM), and by the p38 MAPK inhibitor SB 203580 (10 μM). Furthermore, hypertonic cell shrinkage elicited a biphasic increase in p38 MAPK phosphorylation, with the first significant increase detectable 2 minutes after the hypertonic challenge. Neither myosin light chain kinase-specific concentrations of ML-7 (IC_{50} 40 μM) nor ERK1/2 inhibition by PD 98059 (50 μM) had any effect on NHE activation. Under isotonic conditions, the serine/threonine protein phosphatase inhibitor calyculin A elicited an EIPA- and HOE 642-inhibitable intracellular alkalinization, indicating NHE1 activation. Similarly, shrinkage-induced NHE activation was potentiated by calyculin A. The calyculin A-induced alkalinization was not associated with an increase in the free, intracellular calcium concentration, but was abolished by chelerythrine. It is concluded that shrinkage-induced NHE activation is dependent on PKC and p38 MAPK, but not on MLCK or ERK1/2. NHE activity under both iso- and hypertonic conditions is increased by inhibition of serine/threonine phosphatases, and this effect appears to be PKC-dependent.

Key words: NHE isoforms — Volume regulation — PKC — MLCK — ERK1/2 — P38 MAPK — Protein phosphatases

Introduction

Seven mammalian Na^+/H^+ exchanger (NHE) isoforms, NHE1-7, differing with respect to distribution pattern and regulation, have been cloned and characterized to date (Counillon & Pouyssegur, 2000; Wakabayashi, Shigekawa, & Pouysségur, 1997; Numata & Orlowski, 2001). Most tissues studied express several NHE isoforms. NHE1 is ubiquitously expressed in mammalian cells, and is, in polarized cells, mainly localized to the basolateral membrane (*see* Wakabayashi et al., 1997). NHE2 and NHE3 are predominantly found in epithelial cells, with high expression in kidney, intestine, and stomach. NHE2 is most commonly localized to the apical membrane (e.g., Hoogerwerf et al., 1996; *see* Wakabayashi et al., 1997), although a basolateral localization has also been reported (Soleimani et al., 1994). NHE3 is found both on the apical membrane and in endomembrane compartments (Janecki et al., 1998). NHE4 and NHE5 exhibit the highest expression in the stomach, brain, and kidney (*see* Wakabayashi et al., 1997; Rossmann et al., 2001; Attaphitaya, Nehrke, & Melvin, 2001), and NHE6 and NHE7 appear to be exclusively intracellular, localized to mitochondria and to the trans-Golgi network, respectively (*see* Counillon & Pouyssegur, 2000; Numata & Orlowski, 2001).

The NHEs play important roles in a range of physiological processes, including the regulation of cellular volume and pH, and the transepithelial transport of NaCl, $NaHCO_3$, and NH_4^+ (*see* Wakabayashi et al., 1997; Counillon & Pouyssegur,

*Contributed equally to this paper.

Correspondence to: E.K. Hoffmann; email: ekhoffmann@aki.ku.dk

2000). Ehrlich ascites tumor cells (EATC) exhibit amiloride-sensitive Na^+/H^+ exchange in response to a variety of stimuli, such as intracellular acidification (Kramhøft, Lambert, & Hoffmann, 1988), stimulation with Ca^{2+}-mobilizing agonists, including ATP (Wiener, Dubyak, & Scarpa, 1986; Pedersen et al., 1998a), thrombin, bradykinin (Pedersen, Jørgensen, & Hoffmann, 1998b), and LPA (Pedersen et al., 2000), and hypertonic cell shrinkage (Levinson, 1991; Pedersen et al., 1996). However, the molecular identity and localization of the NHE isoforms in EATC, as well as their relative contributions to Na^+/H^+ exchange after various stimuli, are so far unknown.

Several lines of evidence suggest that serine/threonine phosphorylation events play an important role in the regulation of NHE1. Thus, ATP is required for optimal NHE1 function, although not always reflecting a requirement for direct NHE1 phosphorylation (*see* Wakabayashi et al., 1997), and activation of NHE1 by a range of stimuli is inhibited by serine/threonine protein kinase inhibitors, and activated or stimulated by serine/threonine protein phosphatase inhibitors (Bianchini et al., 1991; Sardet, Fafournoux, & Pouyssegúr, 1991; *see* Malapert et al., 1997; Wakabayashi et al., 1997). We have previously found that at 25°C, the serine/threonine phosphatase inhibitor calyculin A (CL-A) stimulates shrinkage-induced NHE activity in EATC, but does not elicit isotonic NHE activation, but the mechanism involved was not further investigated (Pedersen et al., 1996).

The NHE isoforms are differentially sensitive to osmotic stress. Osmotic cell shrinkage activates NHE1, NHE2, and NHE4 (*see* Wakabayashi et al., 1997; *see also* Nath et al., 1996 for a different view on NHE2), whereas it inhibits NHE3 (Kapus et al., 1994; Nath et al., 1996) and NHE5 (Attaphitaya et al., 2001). The signal transduction mechanisms leading to NHE activation by cell shrinkage remain incompletely understood. Multiple protein kinases are activated following hypertonic stress in mammalian cells, including several protein kinase C (PKC) isoforms (Larsen et al., 1994; Zhuang, Hirai, & Ohno, 2000; Miyata et al., 2001), myosin light chain kinase (MLCK) (Klein & O'Neill, 1995; Krarup et al., 1998) and the mitogen-activated protein kinase (MAPK) subfamilies ERK1/2, P38 MAPK, and JNK/SAPK (Pandey et al., 1999; Roger et al., 1999; Duzgun et al., 2000; Gillis et al., 2001). In EATC, rapid, shrinkage-induced activation has been directly demonstrated for PKC (Larsen et al., 1994), and strongly suggested for MLCK (Krarup et al., 1998).

Evidence regarding the possible roles of specific serine/threonine protein kinases in the shrinkage-induced NHE activation is, however, limited and often conflicting. In EATC (Pedersen et al., 1996), but not in lymphocytes (Grinstein et al., 1985a; Grinstein, Elder, & Furuya, 1985b), a PKC isoform appears to play a role in this process. A role for MLCK in shrinkage-induced NHE activation has been proposed in rat astrocytes (Shrode et al., 1995) and in C6 cells (Shrode et al., 1997). As for the MAPK family, a role for JNK in the hypertonic activation of a *Xenopus laevis* NHE activity has recently been reported (Goss et al., 2001). Roles for ERK1/2 and p38 MAPK in NHE1 activation by other stimuli have been demonstrated (Bianchini, L'Állemain, & Pouyssegúr, 1997; Khaled et al., 2001), as has the involvement of p38 MAPK in the regulatory volume increase (RVI) process (Roger et al., 1999; Sheikh-Hamad et al., 1998), but available evidence has so far argued against a role for either of the MAPK subfamilies in the shrinkage-induced NHE1 activation in mammalian cells.

Consequently, the aims of the present study were, firstly, to establish which NHE isoforms are present in EATC and determine their subcellular localization, and secondly, to further elucidate the role of protein phosphorylation-dephosphorylation events in NHE regulation under iso- and hypertonic conditions. It is concluded that NHE1, NHE2, and NHE3 are all present in EATC, with different subcellular localization patterns. The shrinkage-induced NHE activation is dependent on PKC and p38 MAPK, but not on MLCK or ERK1/2. NHE activity is increased under both iso- and hypertonic conditions by inhibition of serine/threonine phosphatases, and this effect appears to be counteracted by inhibition of PKC.

Part of these results has previously been presented in abstract form (Varming, Pedersen, & Hoffmann, 1998).

Materials and Methods

Reagents

Unless otherwise stated, all reagents were of analytical grade and obtained from Sigma (St. Louis, MO) or Mallinckrodt Baker B.V. (Deventer, Netherlands). Heparin was from Leo (Ballerup, DK). ML-7 was from Calbiochem (Bad Soden, Germany), and was dissolved at 5 mM in 96% ethanol. Gö 6850, Gö 6976, SB 203580 and PD 098059 were also from Calbiochem and were dissolved at 1, 0.5, 2 and 20 mM, respectively, in desiccated DMSO. Calyculin A and chelerythrine were from Alomone Laboratories (Jerusalem, Israel), and were dissolved at 20 μM in 96% ethanol, and at 2.5 mM in ddH_2O, respectively. HOE 642 (a kind gift from Dr. W. Scholz, Merck, Darmstadt, Germany) was dissolved at 0.5 mM in ddH_2O. EIPA was from Molecular Probes (Leiden, the Netherlands), and was dissolved at 2.5 mM in ddH_2O. Fura-2-AM and BCECF-AM, also from Molecular Probes, were dissolved at 10 and 1.2 mM, respectively, in desiccated DMSO. Poly-L-lysine (250 mg/ml) was dissolved in ddH_2O, and nigericin (1 mg/ml) in 96% ethanol. All these reagents were stored at −20°C until use. Stock solutions of paraformaldehyde (20% w/v in ddH_2O) were prepared fresh regularly, and kept at 4°C.

Media and Cell Suspensions

Standard medium contained (in mM) 143 NaCl, 5 KCl, 1 $MgSO_4$, 1 Na_2HPO_4, 1 $CaCl_2$, 3.3 MOPS, 3.3. TES, and 5 HEPES. NaOH was used to adjust pH to 7.4. The hypertonic (600 mOsm) medium was prepared by doubling the concentrations of all ions except Ca^{2+} compared to the standard medium (310 mOsm), while maintaining the same concentrations of MOPS, TES and HEPES. In the p38 Western blot experiments, the hypertonic medium was prepared by addition of NaCl to a final osmolarity of 600 mOsm. In KCl medium, KCl was substituted for NaCl in equimolar amount, and pH was adjusted with KOH.

Ehrlich ascites tumor cells (EATC, hyperdiploid strain) were maintained in NMRI mice by weekly intraperitoneal transplantation. One week after transplantation, the cells in the ascites fluid were harvested in standard incubation medium with added heparin (2.5 IU/ml), as described previously (Hoffmann, Lambert, & Simonsen, 1986). The cells were washed 2–3 times in heparin-free standard medium by centrifugation (700× g, 45 sec), and resuspended at a cytocrit of 4–8%. Prior to experiments, the cells were incubated for 15–30 min in the standard medium, in a water bath with gentle shaking. Unless otherwise indicated, experiments were carried out at 37°C.

NHE Isoform Identification and Localization

Polyclonal primary antibodies recognizing the C-terminal ends of NHE1 (ab 1950), NHE2 (ab 597), or NHE3 (ab 1380), respectively, were a generous gift from Dr. M. Donowitz, Johns Hopkins University, USA. The antibodies have been described previously, and are known to exhibit essentially no cross-reactivity between isoforms (Tsé et al., 1994b; Hoogerwerf et al., 1996).

For SDS-PAGE and Western blotting, crude cell membranes were prepared by pelleting cell aliquots, followed by resuspension in stabilization buffer (62.5 mM Tris, 138.6 mM SDS, 18% glycerol), boiling for 5 min, and homogenization through 27-G and 18-G syringes. Samples (45 μg protein) were diluted 1:1 in double Laemmli buffer, boiled 5 min, resolved by SDS-PAGE gel electrophoresis, and electrotransferred onto nitrocellulose membranes. Membranes were blocked for 1 hr at room temperature (150 mM NaCl, 13 mM Tris, 5% nonfat dry milk), and incubated with primary antibodies (1:1000 in blocking buffer) overnight at 4°C and then for 1 hr at room temperature. The membranes were washed (150 mM NaCl, 13 mM Tris, 0.02% Triton X-100), incubated for 2 hr with horseradish peroxidase (HRP)-conjugated goat anti-rabbit secondary antibody (1:3000), washed, and bound secondary antibody was detected by enhanced chemiluminescence (ECL) (Amersham, Buckinhamshire, England), in some experiments, the reducing agents dithiothreitol (DTT, 0.2 M) or mercaptoethanol (2%) were added to the solubilization buffer.

For immunolocalization experiments, cell aliquots were paraformaldehyde-fixed as described previously (Pedersen et al., 1999) and allowed to settle on clean, poly-L-lysine-coated no. 1 coverslips. Cells were permeabilized for 10 min with 0.02% Triton X-100 in TBS (in mM: 150 NaCl, 10 Tris HCl, 1 $MgCl_2$, 1 mM EGTA, pH 7.4, and, unless otherwise indicated, 0.1% w/v azide), followed by three washes in TBS, blocking for 1 hr with normal goat serum (1:10 in TBS with 1% w/v BSA), incubation for 1 hr with primary antibody (1:1000 in TBS with 1% w/v BSA), three washes in TBS with 1% w/v BSA, incubation for 1 hr with FITC-conjugated goat anti-rabbit IgG (Sigma Immunochemicals, 1:1000 in TBS with 1% w/v BSA), and four washes in TBS with 1% w/v BSA. Samples were mounted on glass slides with spacers to prevent compression (mounting medium: 10% TBS, 90% glycerol, 0.6 mg/l DABCO), and viewed using a 40×/1.25 NA plan apochromat objective mounted on a Leica DM IRB/E microscope coupled to a Leica TSC NT confocal laser scanning unit (Leica Lasertechnik, Heidelberg, Germany). Excitation- and emission wavelengths were 488 nm and 520 nm, respectively, optical slice thickness was 1 μm, and images were frame-averaged.

Estimation of P38 MAPK Phosphorylation

After harvesting as above, EATC were pelleted at 700× g for 45 sec and resuspended at cytokrit 4% in a 5-ml volume of either isotonic standard medium or in hypertonic medium (600 mOsm) for 15 sec, 1, 2, 3, 10 or 30 min. Two hundred-μl volumes of cell suspension were then transferred to 200 μl boiling lysis buffer (2% SDS, 20 mM TRIS pH 7.4, 0.1% Tween-20, 2 mM orthovanadate) for 5 min followed by 3 × 15-sec sonication. Cell homogenates were centrifuged at 20,000× g for 5 min at 4°C, and protein concentration in 2-μl aliquots of supernatants with solubilized proteins was determined with a DC protein assay (BIO-RAD) using the GeneQuant *pro* (Pharmacia). Proteins in samples (60 μg of protein) were resolved under denaturing and reducing conditions (SDS-PAGE) according to NuPAGE (10% NuPAGE Bis-TRIS with NuPAGE MOPS SDS Running Buffer [NP0002]) and TRIS-glycine (12%) minigel procedures for the NOVEX Xcell (E19001) system (NOVEX, San Diego, CA). MARK12™ (NOVEX) were used as molecular mass markers. Resolved proteins were stained with Coomassie brilliant blue, and gels were dried with Dry Ease™ Drying System from NOVEX (NI2387) according to the manufacturers instructions. Resolved profiles and molecular mass markers were electrophoretically transferred from SDS-PAGE gel onto nitrocellulose membranes according to the NOVEX Western transfer apparatus instructions for the NOVEX blot module (E19051), Membranes were blocked overnight in blocking buffer, TBST (pH 7.5) with 5% nonfat milk at 4°C, followed by incubation in blocking buffer with a polyclonal rabbit antibody to phosphorylated p38 MAPK (thr180/tyr182) (New England Biolabs, 1:100 in blocking buffer) for 2 hr at room temperature. Binding of primary antibody was detected using alkaline phosphatase (AP)-conjugated goat anti-rabbit IgG secondary antibody (Jackson ImmunoResearch Laboratories) (diluted 1:400 in blocking buffer) and visualized with BCIP/NBT (Kirkegaard & Perry Laboratories, MD). Band intensity was estimated using the Kodak Image Station 440CF and Kodak 1D 3.5.

Estimation of Intracellular pH (pH_i)

Loading of EATC with BCECF-AM and measurement of pH_i were performed essentially as previously described (Pedersen et al., 1996). Briefly, cells were incubated at 37°C with BCECF-AM (3.6 μM) in standard medium (cytocrit 4%), washed twice in standard medium containing BSA (1 mg/ml), and resuspended in this medium at a cytocrit of 8%. The loaded cells were diluted at a cytocrit of 0.3% in the stirred, thermostatted cuvette of a Perkin-Elmer LS-5 luminescence spectrophotometer. Emission was detected at 525 nm after excitation at 445 nm and 495 nm. Extracellular fluorescence (~5–10% of the total signal) was subtracted prior to calculation of the 445 nm/495 nm ratio and linear calibration to pH_i according to (Thomas et al., 1979).

Estimation of the Free, Intracellular Calcium Concentration ($[Ca^{2+}]_i$)

Loading of EATC with fura-2-AM and measurement of $[Ca^{2+}]_i$ were performed essentially as previously described (Jørgensen, Lambert, & Hoffmann, 1996). Cells were incubated at 37°C with

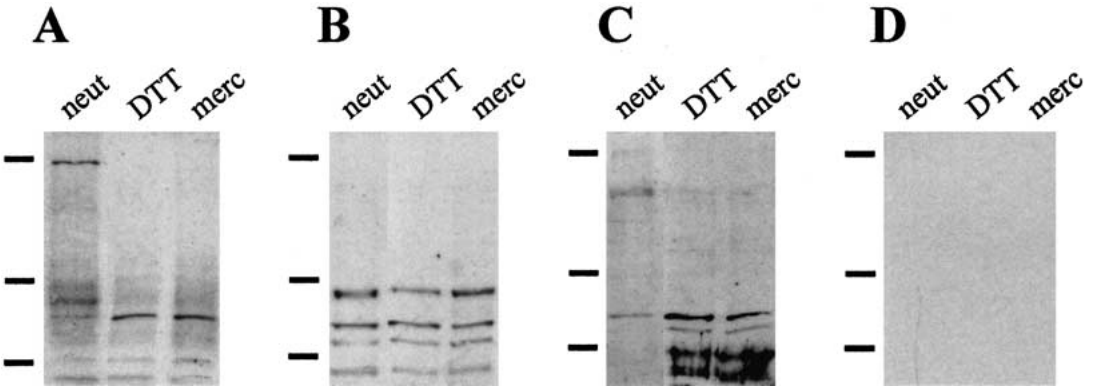

Fig. 1. Western blot analysis of NHE isoforms in Ehrlich ascites tumor cells. Crude membrane fractions from Ehrlich ascites tumor cells (EATC), prepared as described in Materials and Methods, were separated on 6% SDS-polyacrylamide gels and electrotransferred onto nitrocellulose membranes. Membranes were blocked for unspecific labeling, and probed for the presence of the NHE isoforms using rabbit polyclonal antibodies against the C-terminal end of NHE1 (*A*), NHE2 (*B*), or NHE3 (*C*) (1:1000), HRP-conjugated goat anti-rabbit antibody (1:3000), and detection by ECL. In all experiments, labelling in the absence of primary antibody was found to be essentially undetectable (*D*). The horizontal bars represent the positions of molecular weight markers (from top) 202.2, 103.1 and 67.5 kDa. The experiments shown are representative of 4 (NHE1), 4 (NHE2), and 3 (NHE3) independent experiments in the absence, and 2 independent experiments for each isoform in the presence of the reducing agents dithiothretiol (DTT, 0.2 M) and mercaptoethanol (2%).

fura-2-AM (2 μM) in standard medium (cytocrit 4%), washed twice in standard medium containing BSA (1 mg/ml), and resuspended in BSA-free standard medium at a cytocrit of 8%. The loaded cells were diluted at a cytocrit of 0.5% in the stirred, thermostatted cuvette of a PTI Ratiomaster luminescence spectrophotometer. Emission was detected at 510 nm after excitation at 340 nm and 380 nm. Extracellular fluorescence was subtracted prior to calculation of the 340 nm/380 nm ratio, which is used as an estimate of ($[Ca^{2+}]_i$)

Data Analysis and Statistics

The rate of change in intracellular H^+ concentration ($\Delta[H^+]_i$) was calculated from the $[H^+]_i$ at times 0.5 min and 1.5 min after exposure to hypertonic conditions, as ($[H^+]_{i,\ 90\ sec} - [H^+]_{i,\ 30\ sec}$)/60. Data are given as $-\Delta[H^+]_i$ (in $mol \times l^{-1} \times min^{-1}$). As only data obtained under identical osmotic conditions are directly compared, no attempt was made to correct for the intracellular buffering power, which appears to vary relatively little with osmolarity in EATC in the range 310–600 mOsm, as tested in a previous study (Pedersen et al., 1996). The initial pH_i varies between experiments, and NHE activation by cell shrinkage is dependent on pH_i (*see* Fig. 3*B*). Therefore, data were generally calculated relative to the rate from a control experiment with the same initial pH_i, except when all inhibitors used in a given series could be shown to have no effect on initial pH_i. IC_{50} values for inhibition of shrinkage-induced NHE activity were calculated using the equation $y = y_{max} \cdot (1-1(1 + IC_{50}/[\text{inhibitor}]))$, where y and y_{max} are the alkalinization rate at any given concentration of inhibitor, or in the absence of inhibitor, respectively. The only exception to this was the IC_{50} for chelerythrine, which was estimated from the dose-response curve as the concentration required to inhibit the response by 50%, as the datapoints obtained could not be fitted using the above equation.

Abbreviations

BCECF-AM:2′,7′-bis-(2-carboxyethyl)-5,6-carboxyfluorescein, tetraacetoxymethylester; chelerythrine: 1,2-dimethoxy-N-methyl[1,3]benzo-dioxolo[5,6-c]phenanthridinium chloride; DABCO: triethylene diamine; 1, 4 diazabicyclo-[2.2.2]octane; EATC: Ehrlich ascites tumor cells; EGTA: Ethylene glycol-bis(b-aminoethylether)-N,N,N′,N′-tetraacetic acid; EIPA: 5′(*N*-ethyl-*N*-isopropyl)amiloride, hydrochloride; ERK1/2: extracellular signal regulated kinase 1/2; Gö 6850: 1*H*-pyrrole-2,5-dione,3-(1-(3-dimethylamino)propyl)-1*H*-indol-3-yl)-4-(1*H*-indol-3-yl)-[MESH]; Gö 6976: 12*H*-indolo(2,3-*a*)pyrrolo(3,4-*c*)carbazole-12-propanenitrile,5,5,7,13-tetra hydro-13-methyl-5-oxo-[MESH]; HEPES: N-(2-hydroxyethyl)piperazine-N′-2-ethanesulfonic acid; HOE 642:4-isopropyl-3-ethylsulphonylbenzoyl-guanidine methanesulphonate; JNK/SAPK: c-Jun N-terminal kinase/stress activated protein kinase; MARK: mitogen activated protein kinase; MKK1: MAPK kinase 1; ML7: 5-Iodonaphtalene-l-sulfonyl)homopiperazine, hydrochloride; MLCK: myosin light chain kinase; MOPS: 3-(N-morpholino)propanesulfonic acid; NHE: sodium proton exchanger; PD98059: 2′-amino-3′methoxoflavone; PKA: protein kinase A; PKC: protein kinase C; SB203580: 4-(4-fluorophenyl)-2-(4-methylsulfinylphenyl)-5-(4-pyridyl)1H-imidazole; TBS: tris-buffered saline; TES: N-tris(hydroxymethyl)methyl-2-aminoethanesulfonic acid.

Results

Identification of NHE Isoforms NHE1, NHE2, and NHE3 in Ehrlich Ascites Tumor Cells

Western blot analysis of crude membrane fractions was used to analyze for the possible presence of NHE isoforms in the Ehrlich ascites tumor cells (EATC), using polyclonal antibodies raised against the C-termini of NHE1, NHE2, and NHE3 (*see* Materials and Methods). The NHE1 antibody (ab 1950) mainly recognized a protein of about 90 kDa, a few kDa above and below which two additional, weaker bands were visible (Fig. 1*A*). Bands of about

195 kDa and of about 67 kDa or less, respectively, were also detected in most experiments.[1] The NHE2 antibody (ab 597) recognized several proteins of estimated molecular weights 95, 81, 74, and about 67 kDa (Fig. 1*B*). Finally, the NHE3 antibody (ab 1380) recognized a protein of about 84 kDa, and, in some experiments, also a band of about 170 kDa (Fig. 1*C*). In contrast, in experiments in which the reducing agents dithiothreitol (DTT, 0.2 M) or mercaptoethanol (2%) were included in the solubilization buffer to reduce all the NHE protein to the monomer form, the presumed dimer bands were either nondetectable (NHE1) or very weak (NHE3) (compare lane *1* with lanes *2* and *3* in Fig. 1*A* and *C*). No labelling could be detected in the absence of primary antibody (Fig. 1*D*).

Subcellular Localization of NHE1, NHE2, and NHE3

The subcellular localization of NHE1, NHE2, and NHE3 was studied by confocal visualization of fixed, permeabilized EATC, labelled with the same polyclonal antibodies used for Western blot. NHE1-immunolabelling was prominent in the cortical region in or closely adjacent to the plasma membrane, but could also readily be detected in intracellular regions (Fig. 2*A*). Significant NHE2 labelling was seen both in the cortical region and intracellularly, with a "patchy" distribution, suggesting the association of the exchanger with intracellular compartment(s) (Fig. 2*B*). NHE3 labeling exhibited a similar patchy distribution pattern over most of the intracellular compartment, but was essentially absent from the plasma membrane (Fig. 2*C*). In controls, in which primary antibody was omitted, only very faint, diffuse intracellular fluorescence could be detected (Fig. 2*D*).

Effect of Osmotic Cell Shrinkage on NHE Activity

When EATC loaded with the fluorescent pH indicator BCECF were diluted in hypertonic medium (600 mOsm, compared to 310 mOsm isotonic), a rapid intracellular alkalinization was seen after a brief lag time of about 20 sec (Fig. 3*A*). The shrinkage-induced NHE activity was found to correlate inversely and in a sigmoidal fashion with the pH_i measured immediately after hypertonic exposure (Fig. 3*B*). The shrinkage-induced intracellular alkalinization was inhibited by EIPA and HOE 642 with IC_{50} values of 0.19 μM and 0.85 μM, respectively (Fig. 3*C*,*D*), indicating that it mainly reflected activation of NHE1 (*see* Discussion).

Possible Roles of PKC and MLCK in the Shrinkage-induced Activation of NHE

Preincubation with the protein kinase C inhibitor chelerythrine inhibited the shrinkage-induced NHE activation in a concentration-dependent manner, with an IC_{50} value estimated at 12.5 μM (Fig. 4*A*). To further address the possible involvement of PKC, we next tested the effect of two other PKC inhibitors, Gö 6850, which inhibits both the conventional Ca^{2+}-dependent PKC isoforms (α,βI) and the Ca^{2+} independent novel PKC (δ,ε) isoforms, and Gö 6976, which selectively inhibits the conventional PKC isoforms (Martiny-Baron et al., 1993; Way, Chou, & King, 2000) (Fig. 4*B*). As seen, preincubation with Gö 6850 (5 μM, 30 min, $p < 0.002$, $n = 8$) or Gö 6976 (1 μM, 30 min, $p < 0.03$, $n = 8$) inhibited shrinkage-induced NHE activation by about 40% and 30%, respectively.

In contrast, the MLCK inhibitor ML-7 had little effect on the shrinkage-induced NHE activation in EATC (Fig. 4*D*). The IC_{50} for inhibition of shrinkage-induced NHE activity by ML-7 was estimated at 40 μM, compared to reported IC_{50} values of 0.3 μM for MLCK, 21 μM for PKA, and 42 μM for PKC (Saitoh et al., 1987).

Possible Roles of ERK1/2 and p38 MAPK in the Shrinkage-induced Activation of NHE

Figure 5 shows the effect of the MEKK1 inhibitor (i.e., preventing activation of the MEKK1 substrates ERK1/2) PD 098059 (50 μM, 30 min) and the p38 MAPK inhibitor SB 203580 (10 μM, 30 min) on the shrinkage-induced NHE activation. As seen, the initial rate of shrinkage-induced NHE activity is unaffected by pretreatment with PD 098059 ($n = 4$), but is inhibited by about 35% by pretreatment with SB 203580 ($n = 8$, $p < 0.03$), suggesting that p38 MAPK is involved in the activation of NHE by osmotic shrinkage in EATC.

Further supporting this notion, Western blot analysis showed a rapid increase in p38 MAPK phosphorylation, corresponding to activation, after a hypertonic challenge of the same magnitude as that used to elicit NHE activation (Fig. 6). As can be seen, the hypertonic challenge induced a biphasic increase in p38 MAPK phosphorylation in EATC over time, with significantly increased p38 MAPK phosphorylation detectable two min after hypertonic challenge. The phosphorylation appeared to return to control levels at time 5 min, followed by a larger, significant increase again at time 10–30 min after hypertonic challenge.

[1]The poor electrotransfer efficiency of very high molecular weight proteins may explain why the 195 kDa (and for NHE3, 170 kDa) bands were not always detected.

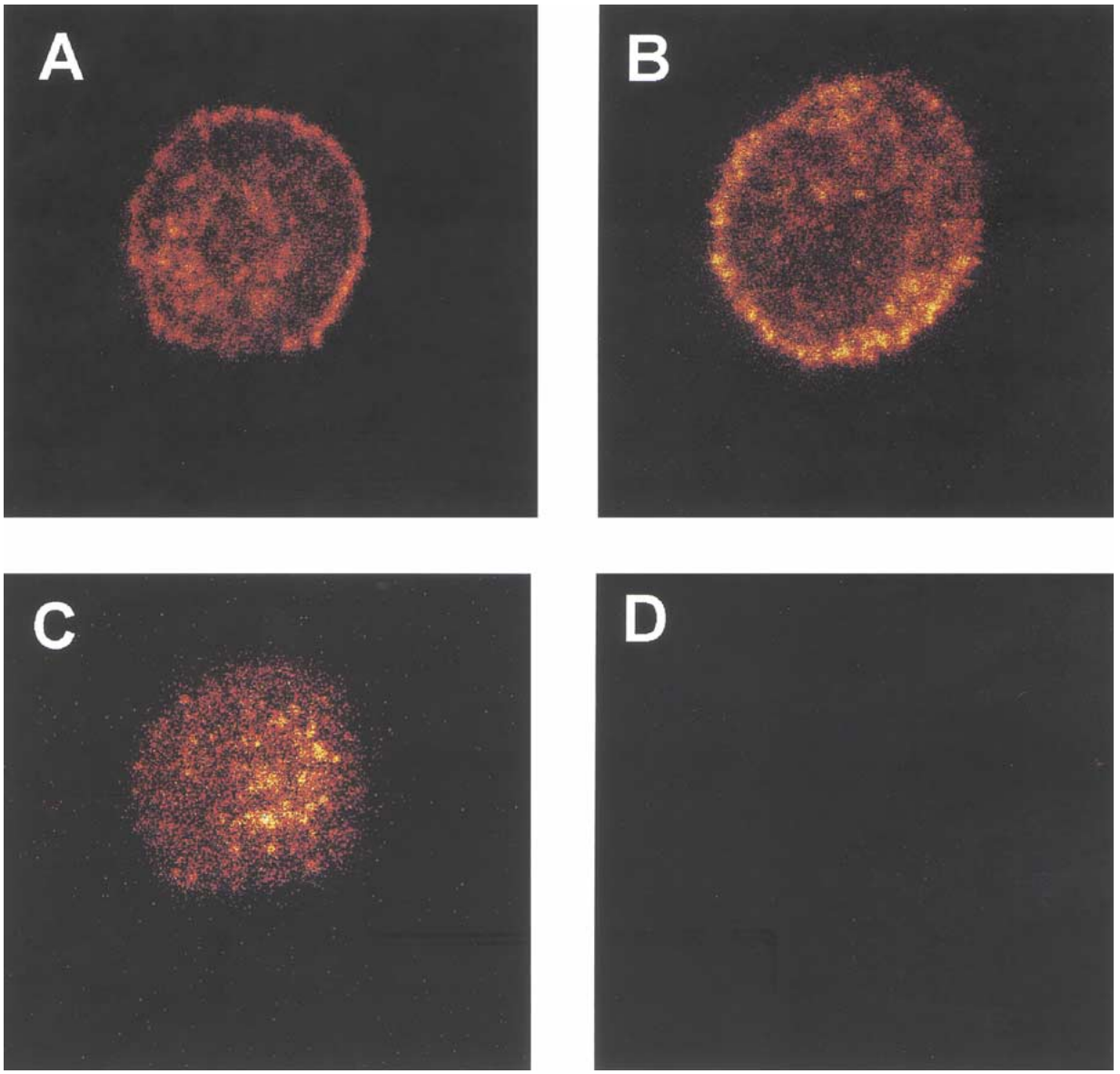

Fig. 2. Subcellular localization of NHE isoforms in EATC. Cells suspended in isotonic standard medium were fixed in 2% paraformaldehyde, washed, allowed to settle on poly-L-lysine coated no. 1 coverslips, and permeabilized using 0.02% Triton X-100. Permeabilized cells were blocked for unspecific labeling, incubated for 1 hr with antibodies against NHE1 (*A*), NHE2 (*B*), or NHE3 (*C*) (1:1000), washed, incubated for 1 hr with FITC-conjugated goat anti-rabbit IgG (1:1000), washed, mounted and viewed using the 488-nm Ar/Kr line of a Leica TSC NT confocal laser scanning unit on a Leica DM IRB/E microscope (for details, *see* Materials and Methods). In the absence of primary antibody, no (*D*) or only very faint, diffuse intracellular fluorescence could be detected. The experiments shown are representative of four independent experiments for each isoform.

Effect of Calyculin A on NHE Activity in EATC under Isotonic Conditions: Possible Roles of PKC and of Changes in $[Ca^{2+}]_i$

The possible role of serine/threonine protein phosphatases in the regulation of NHE activity under steady-state isotonic conditions was investigated using calyculin A (CL-A), which inhibits PP1 and PP2a with in vitro inhibition constants in the nanomolar range (Takai et al., 1995). Figure 7*A* illustrates pH_i over time in EATC suspended in isotonic standard medium (open circles), and after exposure to 100 nM CL-A (filled circles) as indicated by the arrow. As seen, exposure to CL-A resulted in a significant intracellular alkalinization of $7.7 \pm 1.62 \times 10^{-9}$ mol $\times$ $l^{-1} \times min^{-1}$, preceded by a lag time of about 2 min ($n = 11$). The CL-A-induced intracellular alkalinization was abolished in the presence of either

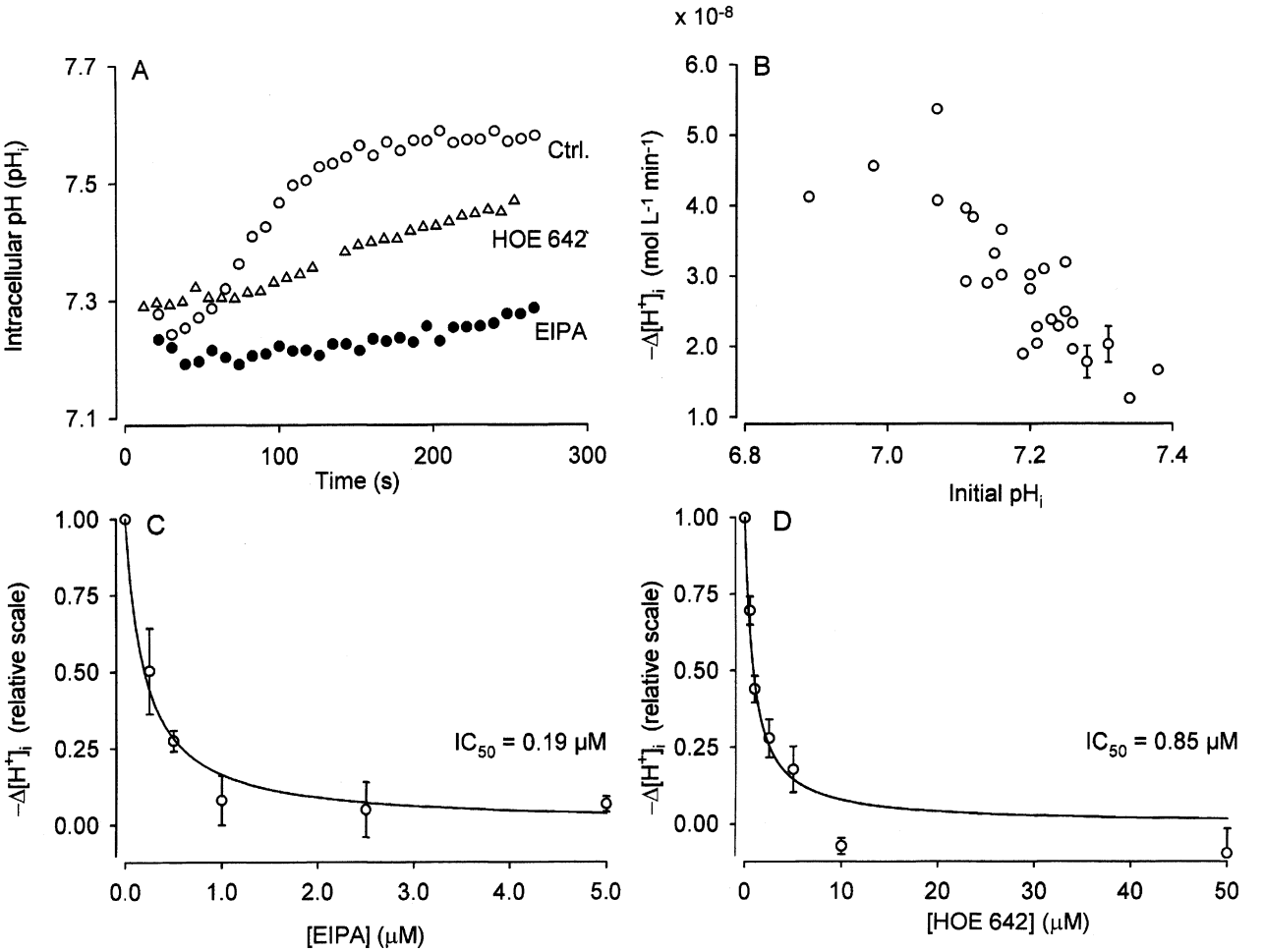

Fig. 3. Activation of NHE by osmotic cell shrinkage: effects of pH_i, EIPA, and HOE 642. (*A*) Activation of NHE by osmotic cell shrinkage. BCECF-loaded cells were diluted in hypertonic (600 mOsm) medium in the thermostatted (37°C) spectrophotometer cuvette at time zero, and pH_i was monitored over time as described in Materials and Methods, under control conditions (○), or in the presence of 5 μM EIPA (●) or HOE 642 (△). The data shown are representative of 45 (*ctrl.*), 4 (*EIPA*), and 4 (*HOE 642*) separate experiments, respectively. (*B*) Dependence of NHE activation on pH_i. The figure illustrates the relationship between the pH_i measured immediately after dilution of the cells in the cuvette, and the rate of decrease in $\Delta[H^+]_i$ (i.e., intracellular alkalinization) from time 0.5–1.5 min, i.e., after NHE activation. Data shown are calculated from the experiments shown in (*A*) and each data point represents a single experiment, except when two experiments happened to have the same pH_i. (*C*) Effect of EIPA on shrinkage-induced NHE activation. The experimental procedure was as in (*A*) with EIPA present from time zero at the concentration indicated. Data are calculated relative to a control experiment with the same initial pH_i (for details, *see* Materials and Methods). IC_{50} values for inhibition of shrinkage-induced NHE activity were calculated using the equation $y = y_{max} \cdot (1-1/(1 + IC_{50}/[\text{inhibitor}]))$, where y and y_{max} are the alkalinization rate at any given concentration of inhibitor, or in the absence of inhibitor, respectively. Data shown are means with SEM error bars. The number of independent experiments is 5 for 1 μM EIPA, and 4 for all other concentrations. (*D*) Effect of HOE 642 on shrinkage-induced NHE activation. Experimental procedures and data analysis were as described above, except that HOE 642 instead of EIPA was present from time zero at the concentration indicated. Means with SEM error bars are shown. The number of independent experiments is 4 for 5 μM HOE 642, and 3 for all other concentrations.

EIPA (5 μM, $n = 3$, Fig. 7*B*), indicating that it predominantly reflected activation of NHE1. Pre-incubation with chelerythrine (15 μM, 14 min) completely prevented the CL-A-induced NHE1 activation (Fig. 7*B*), suggesting that CL-A may exert its effect on NHE1 activity by inhibiting the dephosphorylation of a PKC substrate(s). Finally, exposure to 100 nM CL-A did not elicit a detectable increase in $[Ca^{2+}]_i$ in EATC suspended in isotonic standard medium (Fig. 7*C*, $n = 6$), arguing against a role for detectable $[Ca^{2+}]_i$ increases in the effect of CL-A on NHE1.

Effect of CL-A on Shrinkage-induced NHE Activity

The effects of CL-A on NHE activity under hypertonic conditions are illustrated in Fig. 8. As seen in Fig. 8*A* and quantified in Fig. 8*B*, the rate of shrinkage-induced intracellular alkalinization was increased by 60% in the presence of CL-A (100 nM) ($p < 0.001$, $n = 3$). CL-A treatment also essentially abolished the lag period between hypertonic exposure and exchanger activation ($n = 3$, Fig. 8*A*). Similar to

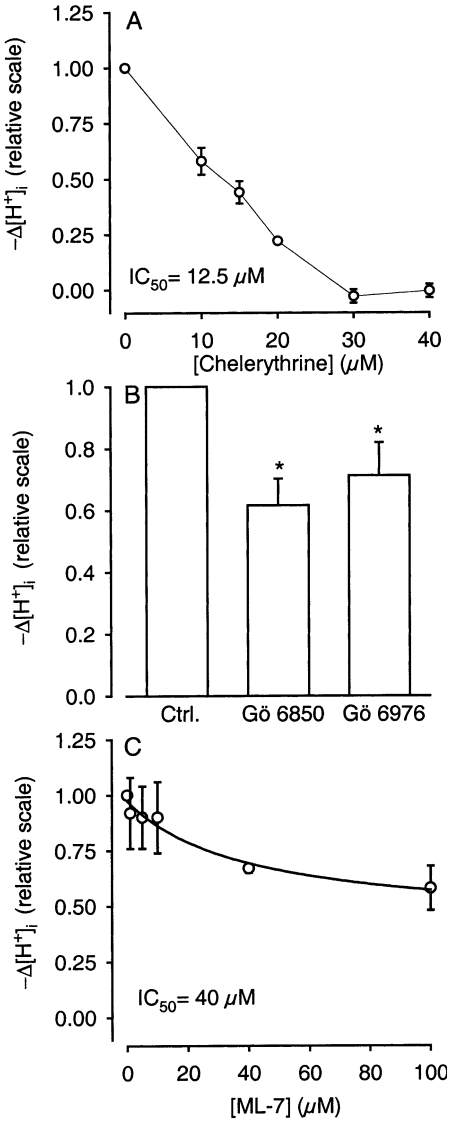

Fig. 4. Effect of inhibitors of PKC and MLCK on shrinkage-induced NHE activation. (*A*) Effect of chelerythrine on shrinkage-induced NHE activation. Experimental procedures were as in Fig. 3*A*, except that the cells had been preincubated with chelerythrine at the concentration indicated for 14 min prior to hypertonic exposure, and chelerythrine was present throughout the experiment. Relative $-\Delta[H^+]_i$/min values were calculated as described in the legend to Fig. 3*B*, except that IC_{50} was estimated manually as the concentration required for half-maximal inhibition (for details, *see* Materials and Methods). Data shown are means with SEM error bars, and the number of independent experiments is 5 for the 15-μM concentration, and 3 for all other concentrations. (*B*) Effect of Gö 6850 and Gö 6976 on shrinkage-induced NHE activation. Experimental procedures were as in Fig. 3*A*, except that where indicated, the cells had been pre-incubated with Gö 6850 (5 μM, 30 min) or Gö 6976 (1 μM, 30 min), and these inhibitors were present throughout the experiments. $-\Delta[H^+]_i$/min was calculated as in Fig. 3*B*, and is given relative to the corresponding control experiment. The data shown are means with SEM error bars, of 8 independent experiments for each condition. **P* values are < 0.002 (Gö 6850) and < 0.03 (Gö 6976). (*C*) Effect of ML-7 on shrinkage-induced NHE activation. Experimental procedures were as in *A*, except that the cells had been preincubated with ML-7 at the concentration indicated for 30 min prior to hypertonic exposure, and ML-7 was present throughout the experiment. Relative $-\Delta[H^+]_i$/min values and IC_{50} were calculated as described in the legend to Fig. 3*B*. Data shown are means with SEM error bars. The number of independent experiments is 3 at all concentrations, except at 40 μM, where it is 7.

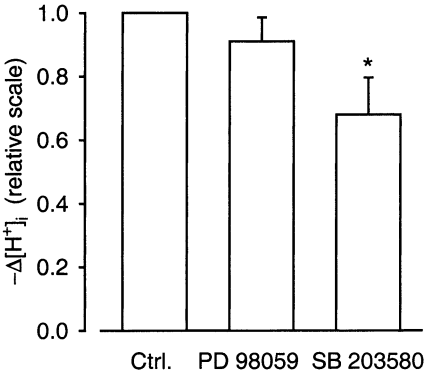

Fig. 5. Possible roles of MAPK subfamilies ERK1/2 and p38 MAPK in the shrinkage-induced NHE activation. (*A*) Effect of the MEKK1 inhibitor PD 98059 and the p38 MAPK inhibitor SB 203580 on shrinkage-induced NHE activation. Experimental procedures were as in Fig. 3*A*, except that where indicated, the cells had been pre-incubated for 30 min with PD 098059 (40 μM), or SB 203580 (10 μM), and these compounds were present throughout the experiment. Relative $-\Delta[H^+]_i$/min values were calculated as described in Fig. 3*B*. Data shown are relative to the corresponding control value, with SEM error bars, of 4 independent experiments for PD 98059 ($p > 0.25$), and 8 independent experiments for SB 203580. *Significantly different from control ($p < 0.03$).

that in the absence of CL-A, the shrinkage-induced NHE activation in the presence of CL-A was inhibited by chelerythrine (Fig. 8*B*).

Discussion

NHE1, NHE2, and NHE3 Presence and Localization in EATC

Ehrlich ascites tumor cells (EATC) have been extensively characterized with respect to NHE function (Kramhøft et al., 1988; Wiener et al., 1986; Levinson, 1991; Pedersen et al., 1996; 1998a; 1998b; Pedersen et al., 2000). The present findings, which strongly indicate that both NHE1, NHE2, and NHE3 are present in EATC, at plasma membrane-intracellular distribution ratios comparable to those reported in other cell types, substantiate the usefulness of these cells as a model system for further studies of NHE function.

NHE1 is an *N*- and *O*-glycosylated protein, resulting in a net molecular weight of 100–110 kDa compared to the calculated molecular weight of about 90 kDa (Counillon, Pouysségur, & Reithmeier, 1994; Shrode et al., 1998; *see* Wakabayashi et al.,

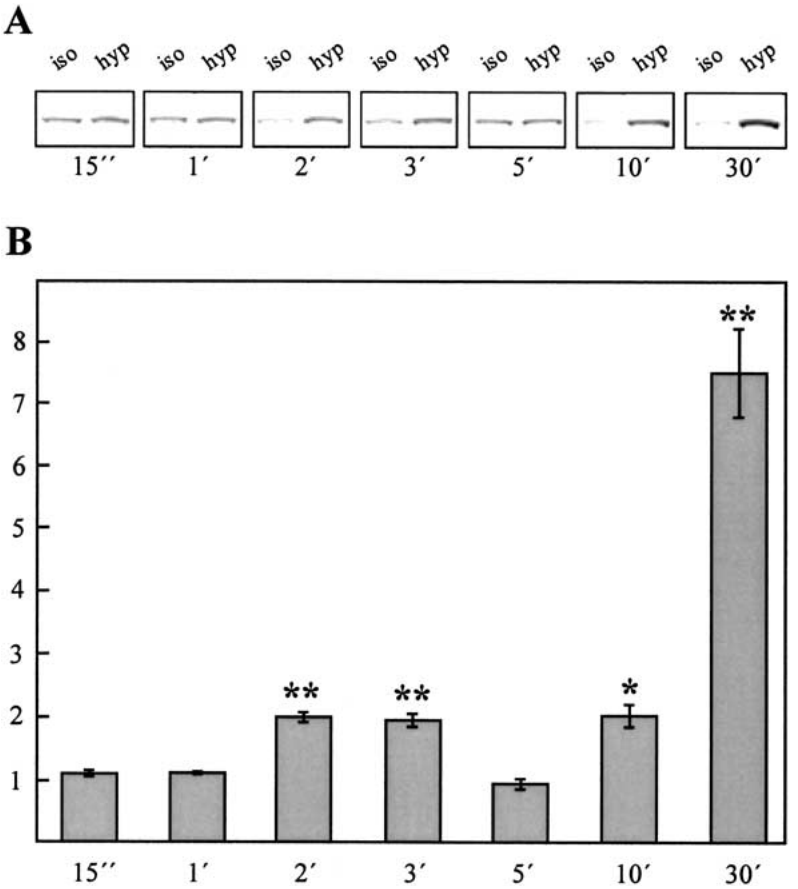

Fig. 6. Western blot analysis of shrinkage-induced changes in the level of p38 MAPK phosphorylation. (*A*) EATC were exposed to isotonic (310 mOsm) or hypertonic (600 mOsm) medium for ~15 sec, 1, 2, 3, 5, 10 or 30 min as indicated below each panel. Crude membrane fractions were prepared as described in Materials and Methods, separated by SDS-PAGE, transferred to nitrocellulose membranes, and labeled with an antibody recognizing phosphorylated p38 MAPK. The experiment shown is representative of 3 independent experiments at each osmolarity. (*B*) Quantitative analysis of increase in time-dependent p38 MAPK phosphorylation intensities of hypertonic challenge relative to isotonic controls. Band intensity relative to that in the corresponding isotonic control was estimated using densitometric software as described in Materials and Methods. * and ** indicate a significant difference from the isotonic control value at the 0.05 and 0.01 level, respectively ($n = 3$).

1997). In Western blots of EATC crude membrane fractions, the most prominent immunoreactive band labelled by the NHE1 antibody had a molecular weight of about 90 kDa, a few kDa above and below which two additional weaker bands could be detected. The lower molecular weight bands most likely correspond to incompletely glycosylated NHE1, consistent with findings in most other cell types studied (e.g. Counillon et al., 1994; Tsé et al., 1994; Shrode et al., 1998; Cavet et al., 1999; Praetorius et al., 2000; *see* Wakabayashi et al., 1997). It has been proposed that immature NHE1 is only seen in significant amounts in cells overexpressing NHE1 (Shrode et al., 1998). However, the present findings, in conjunction with similar recent findings of 80- and 100-kDa NHE1 bands in mouse duodenal epithelial cells (Praetorius et al., 2000), would appear to argue against this notion. The NHE2 antibody labelled four bands with estimated molecular weights of about 67, 74, 81, and 95 kDa, in close agreement with findings in NHE2-transfected PS120 cells (Tsé et al., 1994a), in which it was suggested that the 75-kDa band corresponded to nonglycosylated NHE2 and the 85-kDa band to an *O*-glycosylated form of NHE2. Indeed, multiple bands of molecular weights between 65 and 95 kDa appear to be a general phenomenon for NHE2 in various tissues (Cavet et al., 1999; Hoogerwerf et al., 1996; Praetorius et al., 2000). Given that significant differences between tissues have also been reported for the subcellular localization and regulation of NHE2 (*see* Introduction), it may be speculated that there may in fact be more than one functional form of this isoform. The NHE3 antibody recognized a single .protein of about 84 kDa, in good agreement with findings from other cell types (Hoogerwerf et al., 1996; Cavet et al., 1999; Praetorius et al., 2000). Finally, additional bands of approximately 195 and 170 kDa, respectively, were seen for NHE1 and NHE3, whereas bands in this range were not detected for NHE2 (Fig. 1). These bands were not seen after inclusion of potent reducing agents in the solubilization buffer, and it seems likely that they may represent homodimers. This is in good agreement with previous reports suggesting that both NHE1 and NHE3 can form stable dimers (Fafournoux, Noël, & Pouysségur, 1994). It is, to the knowledge of the authors, not yet clear whether the functional unit for either isoform is a monomer or a dimer (*see* Wakabayashi et al., 1997).

The subcellular localization of the NHE isoforms differed between the three isoforms. In congruence with findings from other cell types (Counillon et al., 1994; D'Souza et al., 1998; Shrode et al., 1998; Cavet et al., 1999), prominent NHE1 labeling was seen

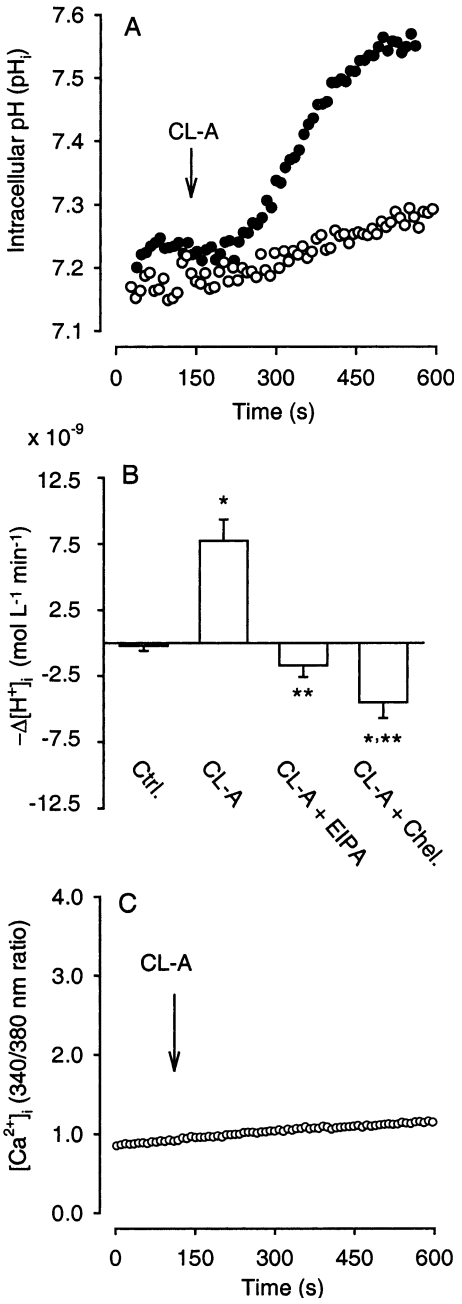

Fig. 7. Effect of calyculin A on NHE activity in EATC under isotonic conditions. (*A*) Effect of calyculin A (CL-A) on pH_i. BCECF-loaded cells were diluted in isotonic (310 mOsm) standard medium in the fluorescence spectrophotometer cuvette at time zero under control conditions (○), or after addition of calyculin A (CL-A, 100 nM) as indicated by the arrow (●). The experiment shown is representative of a total of 11 independent experiments for CL-A and 20 for *ctrl*. (*B*) Effects of EIPA and chelerythrine on the CL-A-mediated decrease in $\Delta[H^+]_i$. The experimental procedure was as in *A*, except that where indicated, EIPA (5 μM) was present from time zero, or chelerythrine (15 μM) was present from 14 min prior to dilution of the cells in the cuvette, and throughout the experiment. The $\Delta[H^+]_i$ was calculated from time 2.0–3.0 min after addition of CL-A, except for the isotonic control value, which changes little with time and was calculated from 0.5–1.5 min after dilution of the cells in the cuvette. Data are means with SEM error bars, of 20 (*Ctrl.*), 11 (*CL-A*), 3 (*CL-A + EIPA*) or 8 (*CL-A + Chel.*) independent experiments. * indicates a significant difference from the isotonic control (p values < 0.0001 for both conditions); ** indicates a significant difference from the value in the presence of CL-A alone (p values < 0.01 for CL-A + EIPA, and < 0.0001 for CL-A + Chel.). (*C*) Effect of CL-A on $[Ca^{2+}]_i$. Fura-2-loaded cells were diluted in isotonic standard medium in the fluorescence spectrophotometer cuvette at time zero. Excitation wavelengths were 340 nm and 380 nm, and emission was measured at 510 nm. CL-A (100 nM) was added as indicated by the arrow. The background-corrected 340 nm/380 nm fura-2 ratio is provided as a measure for $[Ca^{2+}]_i$. The experiment shown is representative of a total of 6 separate experiments.

throughout the plasma membrane. This localization is consistent with kinetic studies, which demonstrated that short-term regulation of this isoform is associated with changes in the K_m for intracellular H^+ rather than with changes in V_{max}, i.e., arguing against a role for recruitment of NHE1 from intracellular stores (e.g., Levine et al., 1993). Intracellular NHE1 labeling was also detectable, probably representing the presence of immature forms of the exchanger in the endoplasmic reticulum or Golgi compartments, as also suggested by other workers (Shrode et al., 1998). The NHE2 antibody labeled epitopes both in the plasma membrane and in intracellular compartments, consistent both with kinetic data indicating regulation of NHE2 by changes in V_{max} (Levine et al., 1993), and with other studies of NHE2 subcellular localization (Cavet et al., 1999; Aharonovitz et al., 2001). Finally, NHE3 was almost exclusively located to the intracellular compartment, in good agreement with the well-documented role of redistribution between the plasma membrane and intracellular compartments in the regulation of this isoform (e.g., D'Souza et al., 1998; Janeckl et al., 1998; Cavet et al., 1999). Interestingly, however, the relative distribution of NHE3 ranges from mainly plasma membrane-associated in Caco-2 cells (Janecki et al., 1998) to almost exclusively intracellular in NHE3-expressing PS120 cells (Cavet et al., 1999).

Cell Shrinkage Predominantly Activates NHE1

Osmotic cell shrinkage elicited a rapid intracellular alkalinization in EATC, previously shown to result from amiloride-sensitive Na^+/H^+ exchange (Levinson, 1991; Pedersen et al., 1996). The shrinkage-induced NHE activity correlated inversely with pH_i in a sigmoidal fashion, presumably due to the allosteric regulation of the transporter by intracellular H^+ (*see* Wakabayashi et al., 1997). The shrinkage-induced NHE activation was inhibited by EIPA and HOE 642 with IC_{50} values of 0.19 μM and 0.85 μM, respectively, suggesting that it predominantly reflected activation of the NHE1 isoform (Wakabayashi et al., 1992; Scholz et al., 1995). Thus, our findings suggest that although NHE2 is present in EATC, it contributes

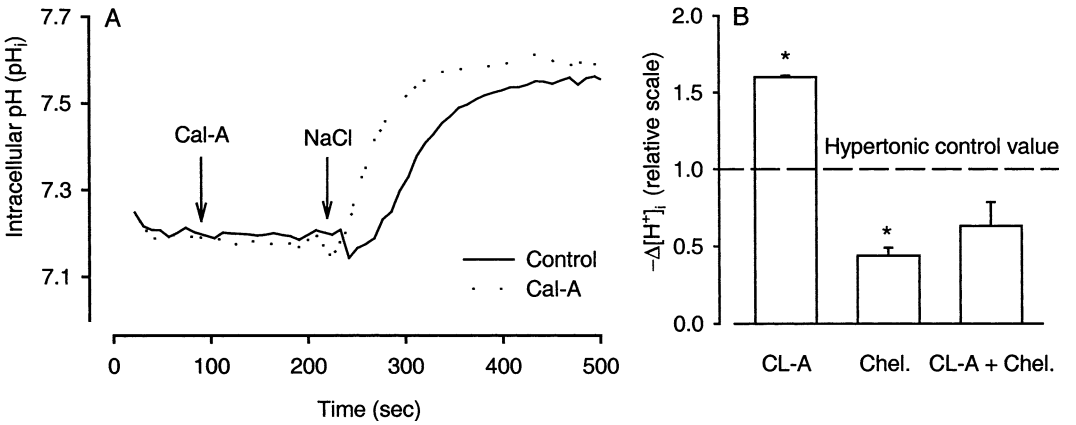

Fig. 8. Effect of CL-A on the shrinkage-induced NHE activation. (*A*) Activation of NHE by osmotic shrinkage in the presence of CL-A. Experimental procedures were as in Fig. 3*A*, except that where indicated, CL-A (100 nM) was present from time zero. The traces shown are representative of 45 (control) and 3 (CL-A) independent experiments. (*B*) Experimental procedures as in panel *A*, except that where indicated, the cells had been pre-incubated with chelerythrine (15 μM, 14 min), in which case both CL-A (100 nM) and chelerythrine (15 μM) were present from time zero. Relative $-\Delta[H^+]_i$/min values from time 0.5–1.5 min were calculated as in Fig. 3*B*. Data are presented as means with SEM error bars, relative to the hypertonic control value for each series, and represent 3 (*CL-A*), 5 (*Chel.*) and 5 (*CL-A + Chel.*) independent sets of experiments. *indicates a significant difference from the corresponding hypertonic control value (*p* values: Ctrl. *vs.* Ctrl. + CL-A: $p < 0.001$; Ctrl. *vs.* Chel.: $p < 0.0005$; Ctrl. *vs.* CL-A + Chel.: $p > 0.05$).

little if any to RVI, in agreement with recent findings in the mucous cells of the rabbit gastric epithelium (Rossmann et al., 2001). Further supporting the conclusion that shrinkage-activated Na^+/H^+ exchange is predominantly NHE1-mediated, NHE3 is not activated by osmotic shrinkage, NHE4 is not inhibited by low EIPA or HOE 642 concentrations, and NHE5 is unlikely to be present in EATC.

Role of Serine/Threonine Protein Kinases in the Shrinkage-induced NHE Activation

PKC

We have previously suggested that at 25°C, PKC plays a role in shrinkage-induced NHE activation in EATC (Pedersen et al., 1996). This appeared somewhat controversial at the time, as studies in human lymphocytes (Grinstein et al., 1986a) and rat astrocytes (Shrode et al., 1995) had argued against a role for PKC in this process. Another issue of concern arose when the specificity of one of the inhibitors used, chelerythrine (Herbert et al., 1990), as a PKC inhibitor was challenged by some (e.g., Lee et al., 1998), although not by other (e.g., Keenan, Goode, & Pears, 1997) recent reports. In the light of this, we have here further addressed the role of PKC. Also at 37°C, shrinkage-induced NHE activation was inhibited by chelerythrine, with an IC_{50} value of 12.5 μM. Moreover, NHE activation was inhibited by the more specific PKC inhibitors Gö 6976, which selectively inhibits the Ca^{2+}-dependent, conventional *c*PKC isoforms, and Gö 6850, which inhibits both *c*PKC (α,βI) and the novel (*n*)PKC (δ,ε) isoforms (Martiny-Baron et al., 1993; *see* Way et al., 2000). At the concentrations used, Gö 6976 should be highly specific for PKC (Martiny-Baron et al., 1993). It can not be entirely excluded that Gö 6850 may have exerted some inhibition of PKA at the concentration used (in vitro IC_{50} 2 μM, Toullec et al., 1991). However, this should if anything lead to an underestimation of the inhibitory effect of Gö 6850, as PKA may slightly inhibit shrinkage-induced NHE activity in EATC, judged from the inhibitory effect of 200 μM 8-Br-cAMP (Pedersen et al., 1994). Thus, the data strongly support our previous conclusion that PKC plays a role in shrinkage-induced activation of NHE in EATC. Both Gö 6850 and Gö 6976 significantly inhibited the response. However, if the effect of Gö 6850 on NHE activity is indeed underestimated, the data may point to the involvement of a Ca^{2+}-independent PKC isoform, consistent with the lack of effect of the Ca^{2+} chelator BAPTA on the response (Pedersen et al., 1996), and the absence of detectable increases in $[Ca^{2+}]_i$ in EATC after osmotic shrinkage (Pedersen et al., 1998b). Supporting this notion, activation of both conventional (*c*), novel (*n*), and atypical (*a*) PKC isoforms by hypertonicity was recently reported in NIH/3T3 cells (Zhuang et al., 2000), and NHE1 activation by the *a*PKC, PKCξ has been directly demonstrated (Sauvage et al., 2000). The discrepancy between our results and those found in lymphocytes (Grinstein et al., 1986a) and astrocytes (Shrode et al., 1995) may reflect differences in shrinkage-induced signalling, as PKC is activated by osmotic cell shrinkage in EATC (Larsen et al., 1994), but not in lymphocytes (Grinstein et al., 1986b). However, it may also be noted that in both of the

above-mentioned studies, the argument was mainly based on PKC depletion using phorbol esters, which would not have downregulated the *a*PKC isoforms such as PKCξ (*see* Hug & Sarre, 1993).

MLCK

In marked contrast to the effect of the PKC inhibitors, the MLCK inhibitor ML-7 only marginally inhibited the shrinkage-induced NHE activation in EATC. The IC_{50} for inhibition of shrinkage-induced NHE activity by ML-7 was about 40 μM, compared to reported IC_{50} values of 0.3 μM for MLCK, 21 μM for PKA, and 42 μM for PKC (Saitoh et al., 1987). Importantly, the high IC_{50} value does not reflect a poor penetration of ML-7 in EATC, as the shrinkage-induced activation of the Na^+, K^+, $2Cl^-$ cotransporter (NKCC) in these cells is inhibited by ML-7 with an IC_{50} value of 0.4 μM, using the same incubation protocol (Krarup et al., 1998). Although a role for MLCK in shrinkage-induced NHE activation in astrocytes was proposed based on an even higher IC_{50} value (56 μM, Shrode et al., 1995), the results presented here strongly argue against the notion that MLCK plays a role in the shrinkage-induced NHE activation in EATC. Rather, the similar IC_{50} values for inhibition of PKC and NHE by ML-7 may substantiate the proposed role of PKC in this process.

MAP Kinases p38 and ERK1/2

ERK1/2, p38 MAPK, and JNK are activated by osmotic shrinkage in many cell types (Pandey et al., 1999; Roger et al., 1999; Duzgun et al., 2000; Gillis et al., 2001; Goss et al., 2001), and ERK1/2 plays an important role in NHE1 activation by several growth factors (e.g., Bianchini et al., 1997). However, the MEKK1 inhibitor PD 98059, which prevents activation of ERK1/2 (Dudley et al., 1995) had no effect on shrinkage-induced NHE activation in EATC, arguing against a role for ERK1/2 in the process. This is in good agreement with findings in other cell types (Bianchini et al., 1997; Roger et al., 1999; Gillis et al., 2001). In contrast, the p38 MAPK inhibitor SB 203580, considered highly specific to p38 MAPK (e.g., Davies et al., 2000), significantly inhibited the shrinkage-induced NHE activation in EATC, indicating that p38 MAPK plays an important role in the activation process. Consistent with this, p38 MAPK was found to be rapidly phosphorylated, i.e., activated, in EATC following hypertonic challenge, in agreement with reports in a range of other cell types (Roger et al., 1999; Duzgun et al., 2000; Gillis et al., 2001). The p38 MAPK phosphorylation appeared to be biphasic, exhibiting a significant increase from time 2 to 3 minutes after hypertonic challenge, followed by a decrease to control levels, and a second and larger increase in the period 10 to 30 minutes after hypertonic challenge. The fast activation is consistent with recent data demonstrating that inhibition of p38 MAPK is required for the rapid, amiloride-dependent (*see* Sun et al., 1990) RVI process in rat inner medullary collecting duct cells (Roger et al., 1999). Other rapid, nongenomic effects of p38 MAPK on NHE1 have also been demonstrated; for instance, trophic factor withdrawal results in rapid, p38 MAPK-dependent phosphorylation and activation of NHE1 in murine pro-B-cells (Khaled et al., 2001). Previous reports in NHE1-expressing PS120 cells (Bianchini et al., 1997) and in U937 cells (Gillis et al., 2001) have argued against a role for p38 MAPK in shrinkage-induced NHE1 activation. However, at least in the former, p38 MAPK was not activated by the osmotic shrinkage (Bianchini et al., 1997). The second increase in p38 MAPK phosphorylation is likely to play a role in longer-term effects of hypertonic challenge. Notably, shrinkage-induced activation of p38 MAPK elicits, within 30 min of shrinkage, the transcriptional upregulation of the serum-and-glucocorticoid-dependent serine/threonine kinase, sgk (Bell et al., 2000, Waldegger et al., 2000), which is chelerythrine-sensitive (Lang et al., 2000). While the rapid time course of shrinkage-induced NHE1 activation seen in the present study is not consistent with a role for the sgk pathway in the fast activation process, this warrants future investigations of whether sgk plays other roles in the shrinkage-induced regulation of NHE1.

Taken together, these findings indicate that PKC and p38 MAPK, but not MLCK or ERK1/2, play important roles in NHE activation by shrinkage in EATC, and thus substantiate the notion that regulation of a given NHE isoform can vary based on the cell type in which it is expressed (*see* e.g. Aharonovitz et al., 2001, and references therein). The possible mechanisms of activation of PKC and p38 MAPK by cell shrinkage have yet to be elucidated. For PKC, documented possibilities include shrinkage-induced changes in F-actin organization (see Pedersen et al., 2001), or cellular hydration status (Giorgione & Epand, 1997), whereas for p38 MAPK, candidate pathways involve the focal adhesion kinase-related tyrosine kinase PYK2 (Pandey et al., 1999) and the small GTP-binding protein cdc42 (Wesselborg et al., 1997).

Inhibition of Serine/Threonine Protein Phosphatases Activates NHE under Isotonic Conditions and Potentiates NHE Activation by Cell Shrinkage

Exposure of EATC to 100 nM of the serine/threonine phosphatase inhibitor calyculin A (CL-A) under isotonic conditions resulted in an EIPA-inhibitable NHE activation, preceded by a lag time of about 2

min. Consistent with the present findings, CL-A has been found to activate NHEβ in trout red blood cells, in a manner apparently involving transporter recruitment to the plasma membrane (*see* Malapert et al., 1997). Moreover, okadaic acid, which inhibits PP2A similarly but PP1 much less potently than CL-A (Takai et al., 1995), phosphorylated and activated NHE in lymphocytes (Bianchini et al., 1991), although the kinase targets involved were not identified.

In the present study, the CL-A-mediated NHE activation was not associated with an increase in $[Ca^{2+}]_i$, but could be completely blocked by the PKC inhibitor chelerythrine. Similarly, the shrinkage-induced NHE activation was potentiated in the presence of CL-A, an effect fully blocked by EIPA and inhibited by chelerythrine. Thus, in both cases, it seems that CL-A predominantly activates the NHE1 isoform, and that the process is dependent on a PKC, most likely one of the Ca^{2+}-independent PKC isoforms. The fact that isotonic NHE activation by CL-A occurs at 37°C (this study), but not at 25°C (Pedersen et al., 1996), may suggest that PKC is partly active under isotonic conditions in EATC at 37 but not at 25°C. CL-A treatment does not cause cell shrinkage in EATC (Krarup et al., 1998), which could secondarily have activated PKC and NHE. CL-A does, however, elicit rapid morphological and cytoskeletal changes in EATC, including prominent plasma membrane blebbing and extensive rearrangement of F-actin and myosin II (Pedersen & Hoffmann, 2001). Preliminary immunofluorescence data indicate that NHE1 is present in high density in the CL-A-induced blebs (S.F. Pedersen, unpublished), but whether NHE1 density at the cell surface is altered by the CL-A treatment has yet to be determined.

In conclusion, NHE1, NHE2, and NHE3 are all present in EATC, with different subcellular localization patterns. The shrinkage-induced NHE activation, which predominantly reflects activation of NHE1, is dependent on PKC and p38 MAPK, but not on MLCK or ERK1/2. NHE activity is increased under both iso- and hypertonic conditions by inhibition of serine/threonine phosphatases, and this effect also appears to be PKC-dependent.

The present work was supported by Danish National Research Council (EKH, grants no. 9601317 and 9801946), and by the Carlsberg Foundation (SFP, grant no. 990209/20-840). The authors are grateful to Prof. Mark Donowitz, Johns Hopkins University, USA, for the kind gift of NHE antibodies, to Birgit Jørgensen and Birthe Juul Hansen for excellent technical assistance, and to Dr. Charlotte Hougaard for critical reading of the manuscript.

References

Aharonovitz, O., Kapus, A., Szaszi, K., Coady-Osberg, N., Jancelewicz, T., Orlowski, J., Grinstein, S. 2001. Modulation of Na^+/H^+ exchange activity by Cl^-. *Am. J. Physiol.* **281:**C133–C141

Attaphitaya, S., Nehrke, K., Melvin, J.E. 2001. Acute inhibition of the brain-specific Na^+/H^+ exchanger isoform 5 by protein kinases A and C and cell shrinkage. *Am. J. Physiol.* **281:**C1146–C1157

Bell, L.M., Leong, M.L.L., Kim, B., Wang, E., Park, J., Hemming, B.A., Firestone, G.L. 2000. Hyperosmotic stress stimulates promoter activity and regulates cellular utilization of the serum- and glucocorticoid-inducible protein kinase (Sgk) by a p38 MAPK-dependent pathway. *J. Biol. Chem.* **275:**25262–25272

Bianchini, L., L'Allemain, G., Pouysségur, J. 1997. The p42/p44 mitogen-activated protein kinase cascade is determinant in mediating activation of the Na^+/H^+ exchanger (NHE1 isoform) in response to growth factors. *J. Biol. Chem.* **272:**271–279

Bianchini, L., Woodside, M., Sardet, C., Pouysségur, J., Takai, A., Grinstein, S. 1991. Okadaic acid, a phosphatase inhibitor, induces activation and phosphorylation of the Na^+/H^+ antiport. *J. Biol. Chem.* **266:**15406–15413

Cavet, M.E., Akhter, S., de Medina, F.S., Donowitz, M., Tse, C.M. 1999. Na^+/H^+ exchangers (NHE1–3) have similar turnover numbers but different percentages on the cell surface. *Am. J. Physiol.* **277:**C1111–C1121

Counillon, L., Pouyssegur, J. 2000. The expanding family of eucaryotic Na^+/H^+ exchangers. *J. Biol. Chem.* **275:**1–4

Counillon, L., Pouysségur, J., Reithmeier, R.A. 1994. The Na^+/H^+ exchanger NHE-1 possesses N- and O-linked glycosylation restricted to the first N-terminal extracellular domain. *Biochemistry* **33:**10463–10469

Davies, S.P., Reddy, H., Caivano, M., Cohen, P. 2000. Specificity and mechanism of action of some commonly used protein kinase inhibitors. *Biochem. J.* **351:**95–105

D'Souza, S., Garcia-Cabado, A., Yu, F., Teter, K., Lukacs, G., Skorecki, K., Moore, H.P., Orlowski, J., Grinstein, S. 1998. The epithelial sodium-hydrogen antiporter Na^+/H^+ exchanger 3 accumulates and is functional in recycling endosomes. *J. Biol. Chem.* **273:**2035–2043

Duzgun, S.A., Rasque, H., Kito, H., Azuma, N., Li, W., Basson, M.D., Gahtan, V., Dudrick, S.J., Sumpio, B.E. 2000. Mitogen-activated protein phosphorylation in endothelial cells exposed to hyperosmolar conditions. *J. Cell Biochem.* **76:**567–571

Fafournoux, P., Noël, J., Pouysségur, J. 1994. Evidence that Na^+/H^+ exchanger isoforms NHE1 and NHE3 exist as stable dimers in membranes with a high degree of specificity for homodimers. *J. Biol. Chem.* **269:**2589–2596

Gillis, D., Shrode, L.D., Krump, E., Howard, C.M., Ruble, E.A., Tibbles, L.A., Woodgett, J., Grinstein, S. 2001. Osmotic stimulation of the Na^+/H^+ exchanger NHE1: relationship to the activation of three MAPK pathways. *J. Membrane Biol.* **181:**205–214

Giorgione, J.R., Epand, R.M. 1997. Role of water in protein kinase C catalysis and its binding to membranes. *Biochemistry* **36:**2250–2256

Goss, G.G., Jiang, L., Vandorpe, D.H., Kieller, D., Chernova, M.N., Robertson, M., Alper, S.L. 2001. "Role of JNK in hypertonic activation of Cl^--dependent Na^+/H^+ exchange in *Xenopus* oocytes." *Am. J. Physiol.* **281:**C1978–C1990

Grinstein, S., Goetz, J.D., Cohen, S., Rothstein, A., Gelfand, E.W. 1985a. Regulation of Na^+/H^+ exchange in lymphocytes. *Ann. N.Y.Acad. Sci.* **456:**207–219

Grinstein, S., Elder, B., Furuya, W. 1985b. Phorbol ester-induced changes of cytoplasmic pH in neutrophils: role of exocytosis in Na^+-H^+ exchange. *Am. J. Physiol.* **248:**C379–C386

Grinstein, S., Mack, E., Mills, G.B. 1986a. Osmotic activation of the Na^+/H^+ antiport in protein kinase C-depleted lymphocytes. *Biochem. Biophys. Res. Commun.* **134:**8–13

Grinstein, S., Goetz-Smith, J.D., Stewart, D., Beresford, B.J., Mellors, A. 1986b. Protein phosphorylation during activation of a Na^+/H^+ exchange by phorbol esters and by osmotic shrinking. Possible relation to cell pH and volume regulation. *J. Biol. Chem.* **261:**8009–8016

Herbert, J.M., Augereau, J.M., Gleye, J., Maffrand, J.P. 1990. Chelerythrine is a potent and specific inhibitor of protein kinase. *C. Biochem. Biophys. Res. Commun.* **172:**993–999

Hoffmann, E.K., Lambert, I.H., Simonsen, L.O. 1986. Separate, Ca^{2+}-activated K^+ and Cl^- transport pathways in Ehrlich ascites tumor cells. *J. Membrane Biol.* **91:**227–244

Hoogerwerf, W.A., Tsao, S.C., Devuyst, O., Levine, S.A., Yun, C.H., Yip, J.W., Cohen, M.E., Wilson, P.D., Lazenby, A.J., Tse, C.M., Donowitz, M. 1996. NHE2 and NHE3 are human and rabbit intestinal brush-border proteins. *Am. J. Physiol.* **270:**G29–G41

Hug, H., Sarre, T.F. 1993. Protein kinase C isoenzymes: divergence in signal transduction. *Biochem. J.* **291:**329–343

Jørgensen, N.K., Lambert, I.H., Hoffmann, E.K. 1996. Role of LTD_4 in the regulatory volume decrease response in Ehrlich ascites tumor cells. *J. Membrane Biol.* **151:**159–173

Janecki, A.J., Montrose, M.H., Zimniak, P., Zweibaum, A., Tse, C.M., Khurana, S., Donowitz, M. 1998. Subcellular redistribution is involved in acute regulation of the brush border Na^+/H^+ exchanger isoform 3 in human colon adenocarcinoma cell line Caco-2. Protein kinase C-mediated inhibition of the exchanger. *J. Biol. Chem.* **273:**8790–8798

Kapus, A., Grinstein, S., Wasan, S., Kandasamy, R., Orlowski, J. 1994. Functional characterization of three isoforms of the Na^+/H^+ exchanger stably expressed in Chinese hamster ovary cells. ATP dependence, osmotic sensitivity, and role in cell proliferation. *J. Biol. Chem.* **269:**23544–23552

Keenan, C., Goode, N., Pears, C. 1997. Isoform specificity of activators and inhibitors of protein kinase C gamma and delta. *FEBS Lett.* **415:**101–108

Khaled, A.R., Moor, A.N., Li, A., Kyungjae, K., Ferris, D.K., Muegge, K., Fisher, R., Fliegel, L., Durum, S.K. 2001. Trophic factor withdrawal: p38 mitogen-activated protein kinase activates NHE1, which induces intracellular alkalinization. *Mol. Cell. Biol.* **21:**7545–7557

Klein, J.D., O'Neill, W.C. 1995. Volume-sensitive myosin phosphorylation in vascular endothelial cells: correlation with Na-K-2Cl cotransport. *Am. J. Physiol.* **269:**C1524–C1531

Kramhøft, B., Lambert, I.H., Hoffmann, E.K. 1988. Na^+/H^+ exchange in Ehrlich ascites tumor cells: activation by cytoplasmic acidification and by treatment with cupric sulphate. *J. Membrane Biol.* **102:**35–48

Krarup, T., Jakobsen, L.D., Jensen, B.S., Hoffmann, E.K. 1998. Na^+-K^+-$2Cl^-$ cotransport in Ehrlich cells: regulation by protein phosphatases and kinases. *Am. J. Physiol.* **275:**C239–C250

Lang, F., Klingel K., Wagner, C.A., Stegen, C., Warntges, S., Friedrich, B., Lanzendörfer, M., Melzig, J., Moschen, I., Steuer, S., Waldegger, S., Sauter, M., Paulmichl, M., Gerke, V., Risler, T., Gamba, G., Capasso, G., Kandolf, R., Hebert, S.C., Massry, S.G., Bröer, S. 2000. Deranged Transcriptional regulation of cell-volume-sensitive kinase hSGK in diabetic nephropathy. *Proc. Natl. Acad. Set. USA* **97:**8157–8162

Larsen, A.K., Jensen, B.S., Hoffmann, E.K. 1994. Activation of protein kinase C during cell volume regulation in Ehrlich mouse ascites tumor cells. *Biochim. Biophys. Acta.* **1222:**477–482

Lee, S.K., Qing, W.G., Mar, W., Luyengi, L., Metha, R.G., Kawanishi, K., Fong, H.H., Beecher, C.W., Kinghorn, A.D., Pezzuto, J.M. 1998. Angoline and chelerythrine, benzophenanthridine alkaloids that do not inhibit protein kinase C. *J. Biol. Chem.* **273:**19829–19833

Levine, S.A., Montrose, M.H., Tsé, C.-M., Donowitz, M. 1993. Kinetics and regulation of three cloned mammalian Na^+/H^+ exchangers stably expressed in a fibroblast cell line. *J. Biol. Chem.* **268:**25527–25535

Levinson, C. 1991. Inability of Ehrlich ascites tumor cells to volume regulate following a hyperosmotic challenge. *J. Membrane Biol.* **121:**279–288

Malapert, M., Guizouarn, H., Fiévet, B., Jahns, R., Garcia-Romeu, F., Motais, R., Borgese, F. 1997. Regulation of Na^+/H^+ antiporter in trout red blood cells. *J. Exp. Biol.* **200:**353–360

Martiny-Baron, G., Kazanietz, M.G., Mischak, H., Blumberg, P.M., Kochs, G., Hug, H., Marme, D., Schachtele, C. 1993. Selective inhibition of protein kinase C isozymes by the indolocarbazole Gö 6976. *J. Biol. Chem.* **268:**9194–9197

Miyata, Y., Asano, Y., Muto, S. 2001. Effects of P-glycoprotein on cell volume regulation in mouse proximal tubule. *Am. J. Physiol.* **280:**F829–F837

Nath, S.K., Hang, C.Y., Levine, S.A., Yun, C.H., Montrose, M.H., Donowitz, M., Tsé, C.-M. 1996. Hyperosmolarity inhibits the Na^+/H^+ exchanger isoforms NHE-2 and NHE-3: an effect opposite to that on NHE-1. *Am. J. Physiol.* **270:**G431–G441

Numata, M., Orlowski, J. 2001. Molecular cloning and characterization of a novel $(Na^+, K^+)/H^+$ exchanger localised to the *trans*-Golgi network. *J. Biol. Chem.* **276:**17387–17394

Pandey, P., Avraham, S., Kumar, S., Nakazawa, A., Place, A., Ghanem, L., Rana, A., Kumar, V., Majumder, P.K., Avraham, H., Davis, R.J., Kharbanda, S. 1999. Activation of p38 mitogen-activated protein kinase by PYK2/related adhesion focal tyrosine kinase-dependent mechanism. *J. Biol. Chem.* **274:**10140–10144

Pedersen, S.F., Kramhøft, B., Jørgensen, N.K., Hoffmann, E.K. 1994. The Na^+/H^+ exchange system in Ehrlich ascites tumor cells. Effects of cell volume, phosphorylation, and calcium. *Acta Physiol. Scand.* **151:**26A

Pedersen, S.F., Kramhøft, B., Jørgensen, N.K., Hoffmann, E.K. 1996. Shrinkage-induced activation of the Na^+/H^+ exchanger in Ehrlich ascites tumor cells: mechanisms involved in the activation and a role for the exchanger in cell volume regulation. *J. Membrane Biol.* **149:**141–159

Pedersen, S.F., Pedersen, S., Lambert, I.H., Hoffmann, E.K. 1998a. P2 receptor-mediated signal transduction in Ehrlich ascites tumor cells. *Biochim. Biophys. Acta.* **1374:**94–106

Pedersen, S.F., Jørgensen, N.K., Hoffmann, E.K. 1998b. Dynamics of Ca_i^{2+} and pH_i in Ehrlich ascites tumor cells after Ca^{2+}-mobilizing agonists or exposure to hypertonic solution. *Pflugers Arch.* **436:**199–210

Pedersen, S., Hoffmann, E.K., Hougaard, C., Lambert, I.H. 2000. Cell shrinkage is essential in lysophosphatidic acid signaling in Ehrlich ascites tumor cells. *J. Membrane Biol.* **173:**19–29

Pedersen, S.F., Hoffmann, E.K., Mills, J.W. 2001. The cytoskeleton and cell volume regulation. *Comp. Biochem. Physiol.* **130:**385–399

Pedersen, S.F., Hoffmann, E.K. 2002. Possible interrelationship between changes in F-actin and myosin II, protein phosphorylation and cell volume regulation in Ehrlich ascites tumor cells. *Exp. Cell Res.* **277:**57–73

Praetorius, J., Andreasen, D., Jensen, B.L., Ainsworth, M.A., Friis, U.G., Johansen, T. 2000. NHE1, NHE2, and NHE3 contribute to regulation of intracellular pH in murine duodenal epithelial cells. *Am. J. Physiol.* **278:**G197–G206

Roger, F., Martin, P.Y., Rousselot, M., Favre, H., Feraille, E. 1999b. Cell shrinkage triggers the activation of mitogen-activated protein kinases by hypertonicity in the rat kidney me-

dullary thick ascending limb of the Henle's loop. Requirement of p38 kinase for the regulatory volume increase response. *J. Biol. Chem.* **274:**34103–34110

Rossmann, H., Sonnentag, T., Heinzmann, A., Seidler, B., Bachmann, O., Vieillard-Baron, D., Gregor, M., Seidler, U. 2001. Differential expression and regulation of Na^+/H^+ exchanger isoforms in rabbit parietal and mucous cells. *Am. J. Physiol.* **281:**G447–G458

Saitoh, M., Ishikawa, T., Matsushima, S., Naka, M., Hidaka, H. 1987. Selective inhibition of catalytic activity of smooth muscle myosin light chain kinase. *J. Blol. Chem.* **262:**7796–7801

Sardet, C., Fafournoux, P., Pouysségur, J. 1991. α-thrombin, epidermal growth factor, and okadaic acid activate the Na^+/H^+ exchanger, NHE-1, by phosphorylating a set of common sites. *J. Biol. Chem.* **266:**19166–19171

Sauvage, M., Maziere, P., Fathallah, H., Giraud, F. 2000. Insulin stimulates NHE1 activity by sequential activation of phosphatidylinositol 3-kinase and protein kinase C zeta in human erythrocytes. *Eur. J. Biochem.* **267:**955–962

Scholz, W., Albus, U., Counillon, L., Gögelein, H., Lang, H.-J., Linz, W., Weichert, A., Schölkens, B.A. 1995. Protective effects of HOE642, a selective sodium-hydrogen exchange subtype 1 inhibitor, on cardiac ischaemia and reperfusion. *Cardiovasc. Res.* **29:**260–268

Sheikh-Hamad, D., Di Mari, J., Suki, W.N., Safirstein, R., Watts, B.A.I., Rouse, D. 1998. p38 kinase activity is essential for osmotic induction of mRNAs for HSP70 and transporter for organic solute betaine in Madin-Darby canine kidney cells. *J. Biol. Chem.* **273:**1832–1837

Shrode, L.D., Klein, J.D., Douglas, P.B., O'Neill, W.C., Putnam, R.W. 1997. Shrinkage-induced activation of Na^+/H^+ exchange: role of cell density and myosin light chain phosphorylation. *Am. J. Physiol.* **272:**C1968–C1979

Shrode, L.D., Klein, J.D., O'Neill, W.C., Putnam, R.W. 1995. Shrinkage-induced activation of Na^+/H^+ exchange in primary rat astrocytes: role of myosin light-chain kinase. *Am. J. Physiol.* **269:**C257–C266

Shrode, L., Gan, B.S., D'Souza, S.J., Orlowski, J., Grinstein, S. 1998. Topological analysis of NHE1, the ubiquitous Na^+/H^+ exchanger using chymotryptic cleavage. *Am. J. Physiol.* **275:**C431–C439

Soleimani, M., Singh, G., Bizal, G.L., Gullans, S.R., McAteer, J.A. 1994. Na^+/H^+ exchanger isoforms NHE-2 and NHE-1 in inner medullary collecting duct cells. Expression, functional localization, and differential regulation. *J. Biol. Chem.* **269:**27973–27978

Sun, A.M., Saltzberg, S.N., Kikeri, D., Hebert, S.C. 1990. Mechanisms of cell volume regulation by the mouse medullary thick ascending limb of Henle. *Kidney Int.* **38:**1019–1029

Takai, A., Sasaki, K., Nagai, H., Mieskes, G., Isobe, M., Isono, K., Yasumoto, T. 1995. Inhibition of specific binding of okadaic acid to protein phosphatase 2A by microcystin-LR, calyculin-A and tautomycin: method of analysis of interactions of tight-binding ligands with target protein. *Biochem. J.* **306:**657–665

Thomas, J.A., Buchsbaum, R.N., Zimniak, A., Racker, E. 1979. Intracellular pH measurements in Ehrlich ascites tumor cells utilizing spectroscopic probes generated in situ. *Biochemistry* **18:**2210–2218

Toullec, D., Pianetti, P., Coste, H., Bellevergue, P., Grand-Perret, T., Ajakane, M., Baudet, V., Boissin, P., Boursier, E., Loriolle, F. 1991. The bisindolylmaleimide GF 109203X is a potent and selective inhibitor of protein kinase C. *J. Biol. Chem.* **266:**15771–15781

Tsé, C.-M., Levine, S.A., Yun, C.H., Khurana, S., Donowitz, M. 1994a. Na^+/H^+ exchanger-2 is an O-linked but not an N-linked sialoglycoprotein. *Biochemistry* **33:**12954–12961

Tsé, C.-M., Levine, S.A., Yun, C.H.C., Brant, S.R., Nath, S., Pouysségur, J., Donowitz, M. 1994b. Molecular properties, kinetics and regulation of mammalian Na^+/H^+ exchangers. *Cell. Physiol. Biochem.* **4:**282–300

Varming, C., Pedersen, S.F., Hoffmann, E.K. 1998. Protein kinases, phosphatases and the regulation of the Na^+/H^+ exchanger in Ehrlich ascites tumor cells. *Acta Physiol. Scand.* **163:**A24

Wakabayashi, S., Sardet, C., Fafournoux, P., Counillon, L., Meloche, S., Pages, G., Pouyssegur, J. 1992. Structure function of the growth factor-activatable Na^+/H^+ exchanger (NHE1). *Rev. Physiol. Biochem. Pharmacol.* **119:**157–186

Wakabayashi, S., Shigekawa, M., Pouyssegur, J. 1997. Molecular physiology of vertebrate Na^+/H^+ exchangers. *Physiol. Rev.* **77:**51–74

Waldegger, S., Gabrysch, S., Barth, P., Fillon, S., Lang, F. 2000. h-sgk serine-threonine protein kinase as transcriptional target of p38/MAP kinase pathway in HepG2 human hepatoma cells. *Cell. Physiol. Biochem.* **10:**203–208

Way, K.J., Chou, E., King, G.L. 2000. Identification of PKC-isoform-specific biological actions using pharmacological approaches. *Trends Pharmacol. Sci.* **21:**181–187

Wesselborg, S., Bauer, M.K.A., Vogt, M., Schmitz, M.L., Schulze-Osthoff, K. 1997. Activation of transcription factor NF-kappaB and p38 mitogen-activated protein kinase is mediated by distinct and separate stress effector pathways. *J. Biol. Chem.* **272:**12422–12429

Wiener, E., Dubyak, G., Scarpa, A. 1986. Na^+/H^+ exchange in Ehrlich ascites tumor cells. Regulation by extracellular ATP and 12-O-tetradecanoylphorbol 13-acetate. *J. Biol. Chem.* **261:**4529–4534

Zhuang, S., Hirai, S.I., Ohno, S. 2000. Hyperosmolality induces activation of cPKC and nPKC, a requirement for ERK1/2 activation in NIH/3T3 cells. *Am. J. Physiol.* **278:**C102–C109